



# Robust Fixed Point Transformation based Proportional-Derivative Control of Angiogenic Tumor Growth

Levente Kovács\*, György Eigner\*, József K. Tar\*\*,  
Imre Rudas\*\*

\* *Physiological Controls Research Center, Research, Innovation and Service Center, Obuda University, Budapest, Hungary (e-mail: {kovacs.levente, eigner.gyorgy}@nik.uni-obuda.hu)*

\*\* *Antal Bejczy Center for Intelligent Robotics, Research, Innovation and Service Center, Obuda University, Budapest, Hungary (e-mail: tar.jozsef@nik.uni-obuda.hu, rudas@uni-obuda.hu)*

**Abstract:** The usability of advanced control methods of physiological processes have been several times demonstrated. Advanced (i.e. MPC) control approaches cope with practical difficulties of limited measurability of the state variables, model-imprecisions, significant inter-patient variability of the available model's parameters and limitations in the sampling frequency of the variables that at least in principle can be directly measured. However, the lack of the necessary information prevents the use of state estimators. Compensation of the effects of the presence of model-imprecisions needs the application of robust control methods or adaptive techniques. The Proportional-Derivative (PD) control completed with Robust Fixed Point Transformation (RFPT)-based adaptive control was invented for tackling such difficulties. The current paper investigates the applicability of this technique in case of angiogenic growth of tumors using different scenarios of tumor volume measurement. Conclusions are drawn on the basis of numerical simulations.

© 2018, IFAC (International Federation of Automatic Control) Hosting by Elsevier Ltd. All rights reserved.

**Keywords:** Adaptive Control, Proportional Controls, Robust Fixed Point Transformation, Banach's Fixed Point Theorem, Tumor Growth.

## 1. INTRODUCTION

In contrast to the classical anti-cancer therapies as chemotherapy and radiotherapy, modern approaches use Targeted Molecular Therapies (TMTs) that fight directly against specific cancer mechanisms (Charlton and Spicer (2016)). Their main advantage consists in their limited side effects. As it is well-known, the growth of tumor cells is limited after reaching a given cell size (Distler et al. (2003)). In further development of the tumor the phenomenon of angiogenesis (i.e. the process of new blood vessel formation) plays essential role. Via inhibiting this process (i.e. antiangiogenesis) the growth of the cancerous cells can be kept at bay (Harris (2003); Ilic et al. (2016)).

The idea leads to a pathophysiological control problem with the aim of determining the appropriate value of inhibitor to be injected automatically. Significant modeling and control efforts were done in the last decades regarding the antiangiogenic tumor control (Michelson and Leith (1997); Hanhfeldt et al. (1999); Ledzewicz and Schättler (2005); Lobato et al. (2016); Drexler et al. (2017a); Klamka et al. (2017); Zhou et al. (2015); Ionescu

et al. (2017)), summarized by the review paper Vasudev and Reynolds (2014). Recently, a minimal model of tumor growth with angiogenic inhibition by Bevacizumab administration has been studied (Drexler et al. (2017c)) and developed (Drexler et al. (2017b)) using the latest medical findings in the field. Czako et al. (2017) studied the use of the same minimal model for a Robust Fixed Point Transformation (RFPT)-based adaptive controller as a first RFPT-based application for tumor growth control in the topic.

Transforming a mathematical problem into a fixed point problem, and subsequently solving it via iteration is not new: it goes back to the 17<sup>th</sup> century's Newton-Raphson method (Ypma (1995)), while nowadays its recent variants have been formulated (Kelley (2003); Deuffhard (2004)). For adaptive control purposes it was introduced as alternative to the Lyapunov function-based approach (Tar et al. (2009)). In a wider sense this approach is based on Banach's fixed point theorem (Banach (1922)). Its essence consists in the fact that in a linear, normed, complete metric space (i.e. Banach-space) contractive maps generate Cauchy sequences that necessarily are convergent due to the completeness of the space. It was demonstrated that the limit of such a self-convergent sequence is the solution of the fixed point problem (Tar et al. (2009); Dineva et al. (2016)).

\* This project has received funding from the European Research Council (ERC) under the European Union's Horizon 2020 research and innovation programme (grant agreement No 679681). Gy. Eigner was supported by the ÚNKP-17-4/I New National Excellence Program of the Hungarian Ministry of Human Capacities.

The RFPT-based approach has the great advantage that it does not require full state estimation: it can work by directly measuring only the controlled variable and knowing the control signal in use. Its applicability was successfully pointed out in case of physiological problems, e.g. type 1 diabetes mellitus (Eigner et al. (2015); Kovács (2017)) in which Proportional-Integral-Derivative (PID) controller was completed with the RFPT approach or anaesthesia control (Dineva et al. (2016)).

The current paper investigates the RFPT approach combined with classical control method, and it is structured as follows. In Section 2 the applied tumor growth model is introduced. In Section 3 the application of the RFPT-based control is described. In Section 4 simulations results are presented, followed by conclusions and further direction possibilities (Section 5).

## 2. ANALYSIS OF THE TUMOR GROWTH MODEL IN USE

The detailed model in use is a third order one and was published in Hanhfeldt et al. (1999). The state variables of the model are the volume of the tumor  $x_1(t)$  [ $mm^3$ ], the volume of the supporting vasculature  $x_2(t)$  [ $mm^3$ ], and the inhibitor serum (Bevacizumab) level  $x_3(t) \equiv g(t)$  [ $mg \cdot kg^{-1}$ ]. The model equations are as follows:

$$\begin{aligned} \dot{x}_1(t) &= -\lambda_1 x_1(t) \log \left( \frac{x_1(t)}{x_2(t)} \right) \\ \dot{x}_2(t) &= b x_1(t) - d x_1^\alpha(t) x_2(t) - \eta x_2(t) g(t) \\ \dot{g}(t) &= -\lambda_3 g(t) + u(t) \end{aligned} \quad (1)$$

where the *control signal* is the input rate of the inhibitor  $u(t)$  [ $mg \cdot kg^{-1} \cdot h^{-1}$ ]. The model parameters are  $\lambda_1 = 0.192/24.0$  [ $h^{-1}$ ],  $b = 5.85/24.0$  [ $h^{-1}$ ],  $d = 0.0087/24.0$  [ $mm^{-2} \cdot h^{-1}$ ],  $\eta = 0.66/24.0$  [ $mm^{-3} \cdot h^{-1}$ ],  $\lambda_3 = 1.3/24.0$  [ $h^{-1}$ ], and  $\alpha = 2/3$ .

The aim is to control  $x_1(t)$  by the use of the signal  $u(t)$  and assuming that  $x_1(t)$  is directly measurable. To determine the relative order of the control task we have to observe that  $\dot{x}_1(t)$  is not directly influenced by  $u(t)$ . It is evident that  $\ddot{x}_1(t)$  depends on  $\dot{x}_2(t)$  that directly depends on  $\dot{g}(t)$  what is influenced by  $u(t)$ . As a consequence, the relative order of our task is 3. To reveal the dependence of  $\ddot{x}_1(t)$  on  $u(t)$ , by making the necessary differentiations we arrive to the cascade equations as follows:

$$\begin{aligned} \ddot{x}_1(t) &= -\lambda_1 \dot{x}_1(t) \log \left( \frac{x_1(t)}{x_2(t)} \right) - \lambda_1 \dot{x}_1(t) + \lambda_1 \frac{x_1(t)}{x_2(t)} \dot{x}_2(t) \\ \ddot{x}_1(t) &= \dot{x}_1(t) \left[ -\lambda_1 \log \left( \frac{x_1(t)}{x_2(t)} \right) - \lambda_1 \right] - \lambda_1 \frac{\dot{x}_1^2(t)}{x_1(t)} - \\ &- \lambda_1 \frac{\dot{x}_1(t) \dot{x}_2(t)}{x_2(t)} + \lambda_1 \left( \frac{\dot{x}_1(t)}{x_2(t)} - \frac{x_1 \dot{x}_2(t)}{x_2^2(t)} \right) \dot{x}_2(t) \\ &+ \lambda_1 \frac{x_1(t)}{x_2(t)} (b \dot{x}_1(t) - d \alpha x_1(t)^{\alpha-1} \dot{x}_1(t) x_2(t) \\ &- d x_1^\alpha(t) \dot{x}_2(t) - \eta \dot{x}_2(t) g(t)) + \lambda_1 \eta x_1(t) \lambda_3 g(t) \\ &- \lambda_1 \eta x_1(t) u(t) \end{aligned} \quad (2)$$

that for  $u(t)$  can be summarized in an affine form as follows:

$$\ddot{x}_1(t) = \mathcal{B}(x_1(t), x_2(t), g(t)) - \lambda_1 \eta x_1(t) u(t) \quad (3)$$

where  $\mathcal{B}(x_1(t), x_2(t), g(t))$  represents that all the derivatives of the state variables are determined by themselves. Equations (1) and (2) allow us to observe the followings:

- (1) The  $\frac{0}{0}$  - type singularity in (1) does not allow this model to explain or describe the tumor formation in its early stage that precedes angiogenesis. From this point of view our model is similar to that of the Newtonian classical mechanics that allows us the calculation of the system's trajectory if the initial conditions are known.
- (2) As  $x_1 \rightarrow 0$ ,  $\ddot{x}_1(t)$  becomes insensitive to  $u(t)$  that anticipates, that for keeping the tumor size at very low level it would require the use of huge Bevacizumab ingress rates. In other words, the "Tamed Cancer" concept (i.e. our research concept) is practically reasonable: the aim cannot be the complete removal of the tumor: instead of that it should be kept at a low, but finite level.
- (3) During numerical simulations the physically not interpretable regions as  $x_1(t), x_2(t), g(t) < 0$ , and the physically not realizable ingress rates as  $u(t) < 0$  must be evaded by appropriately completing the equations (1) and (2). The physically clear situation corresponds to a targeted  $x_{1\text{final}} > 0$  state at which these phenomenological restrictions do not occur.
- (4) As we can directly measure only  $x_1(t)$ , but no practical possibility exists for measuring  $x_2(t)$  and  $g(t)$ , the detailed model practically is not available for developing a classical Model Predictive Controller (MPC) (e.g. Grüne and Pannek (2011); Grancharova and Johansen (2012)). By other words, due to the lack of satisfactory information we cannot construct a Kalman filter to estimate each state variable.

This situation ab ovo anticipates the possible use of either some robust controller for a higher relative order task as the Robust Variable Structure / Sliding Mode (VS/SM) Controller (Levant (1998)), or that of some adaptive technique. Since the VS/SM-type controllers normally apply drastic control signals and may cause chattering, in the sequel we concentrate on the use of an PD-RFPT-based adaptive technique.

## 3. APPLICATION OF THE PD-RFPT-BASED TECHNIQUE FOR ANGIOGENIC TUMOR GROWTH

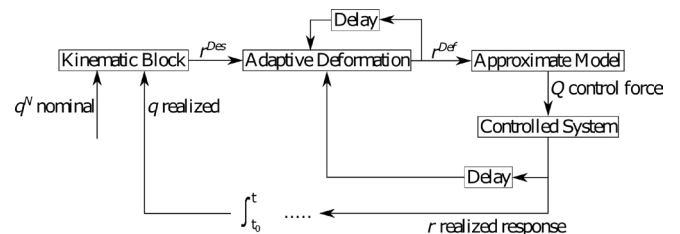


Figure 1. Schematic structure of the Fixed Point Transformation-based Adaptive Controller

According to Fig. 1 describing the schematic structure of the RFPT-based control design, a nominal trajectory to be tracked can be designed for  $x_1^N(t)$  ( $q^N$  in Fig. 1) as follows (Czakó et al. (2017)):

$$x_1^N(t) = x_{1_{final}} + x_{1_{ini}} (1 - \tanh(ct)) \quad (4)$$

where the initial condition corresponds to  $t = 0$ ,  $c > 0$ , and  $x_{1_{final}} > 0$  that guarantees the avoidance of the dynamic singularity of the model.

The PD term is embedded into the Kinematic Block and is responsible for the elimination of the actual tracking error denoted by  $e(t) = x_1^N(t) - x_1(t)$ . Since there is a direct connection between the  $u(t)$  control signal and the third derivative of the first state  $\ddot{x}_1(t)$  we have to use at least a third order  $\left(\frac{d}{dt} + \Lambda\right)^3$  PD term. Taking into account that for a constant  $\Lambda > 0$  the solution of the differential equation  $\left(\frac{d}{dt} + \Lambda\right)h(t) \equiv 0$  converges to zero since it is  $h(t) = h(t_0)\exp(-\Lambda(t - t_0))$ , the tracking error can be used for the prescription of the desired  $\ddot{x}_1^D$  as  $\left(\frac{d}{dt} + \Lambda\right)^3 [x_1^N(t) - x_1(t)] \equiv 0$ , that results in:

$$\ddot{x}_1^D = \ddot{x}_1^N(t) + \Lambda^3 e(t) + 3\Lambda^2 \dot{e}(t) + 3\Lambda \ddot{e}(t) \quad (5)$$

Consequently, the value  $\ddot{x}_1^D$  corresponds to the “Desired Response”  $r^{Des}$  (Fig. 1). In order to achieve this response, following adaptive deformation of the control signal used in the previous control step, the available approximate system model is used for the calculation of the “control force” (denoted by  $Q$  in Fig. 1, which, in our case corresponds to  $u(t)$ ). This force is exerted on the controlled system that produces the “realized response” ( $r$  in Fig. 1,  $\ddot{x}_1(t)$  in our case).

In the case of a digital controller the “Delay” in the figure corresponds to the time resolution of the digital controller. If  $\ddot{x}_1^D$  varies only slowly, an iterative sequence of the control signals  $\{r_1 = r_1^{Des}, \dots, r_{n+1} = G(r_n, f(r_n), r^{Des}), \dots\}$  can be constructed, that, according to Banach’s Fixed Point Theorem, converges to the solution of the control task  $r \equiv f(r_*) = r^{Des}$  if the parameters of the deformation function  $G(r_n, f(r_n), r^{Des})$  are appropriately set. (Here  $f(r)$  is referred as the “response function” of the controlled system that depends on the parameters of the approximate model and the actual system’s properties. Practically, during one digital control step there is a possibility to make a single step of iteration.

In our case the  $F(\xi) = \text{atanh}(\tanh(\xi + D)/2)$  real function with the parameter  $D = 0.3$  was used that has an attractive fixed point at  $\xi_* \approx 0.2594$  used in the FPT:

$$r_{i+1} = \left[ F(A\|f(r_i) - r^{Des}\| + \xi_*) - \xi_* \right] \frac{f(r_i) - r^{Des}}{\|f(r_i) - r^{Des}\|} + r_i \quad (6)$$

applying the concept of the Frobenius norm. In Eq. (6)  $A$  is an adaptive parameter. For  $r_k = r_*$  that provides  $f(r_*) = r^{Des}$  it yields that  $r_{k+1} = r_k$ , meaning that if  $r_*$  is the solution of our task, it is also the fixed point of this function. For achieving convergence parameter  $A$  has to be set appropriately. In the sequel, we investigate the possibilities of increasing the sampling time, i.e. the frequency of measuring of the actual tumor volume  $x_1(t)$ .

### 4. SIMULATION RESULTS

In the first step “ideal possibilities” were assumed for measuring  $x_1$  in each hour ( $\delta t = 1 h$ ). As a result, the time-resolution of the numerical Euler integration was  $1/24 h$ .

For the tracking parameter  $c = \frac{1}{200} h^{-1}$ , and  $A = -6 \frac{h^3}{mm^3}$  with  $x_{1_{final}} = 5^3 mm^3$  and  $\Lambda = 0.015 h^{-1}$  a detailed model was assumed for the calculation of  $\mathcal{B}(x_1(t), x_2(t), g(t))$  in order to obtain information on these possible additive terms. In these simulations the initial values  $x_1(0) = x_2(0) = 10^4 mm^3$  were chosen.

All of the discrete time steps have been selected in accordance to the model properties, measurement technology and physiological realities. To get a full picture, we investigated four scenarios ( $\delta t = [1, 24, 72, 168] h$ ).

The 3<sup>rd</sup> order time-derivatives were estimated as

$$\ddot{x}_1(t) \approx \frac{x_1(t) - 3x_1(t - \delta t) + 3x_1(t - 2\delta t) - x_1(t - 3\delta t)}{\delta t^3} \quad (7)$$

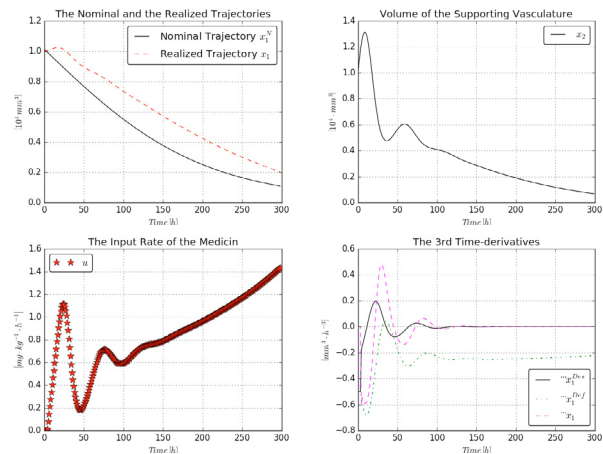


Figure 2. The size of the tumor and its feeding vascular system in the “ideal case”, the ingress rate of the serum Bevacizumab, and the 3<sup>rd</sup> order derivatives

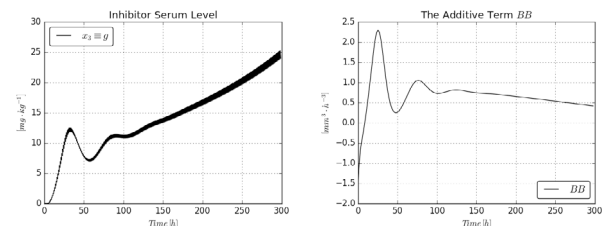


Figure 3. The inhibitor serum level and the additive term  $\mathcal{B}(x_1(t), x_2(t), g(t))$  in the “ideal case”

Figures 2 and 3 reveal the operation of the adaptation: the desired and the “realized” values are in each other’s close vicinity, and they seriously differ from the “deformed” values. The increase in the inhibitor serum level and that in its ingress rate corresponds to our expectation that decreasing  $x_1(t)$  it decreases the sensitivity of the mechanism for the Bevacizumab ingress rate.

Consequently, in further calculations instead of the “exact” model (3) its affine approximation (8) was applied that does not require the measurement of  $x_2(t)$  and  $x_3(t) \equiv g(t)$ . The role of the adaptivity is to compensate the effects of the affine approximation in:

$$\ddot{x}_1(t) = \hat{B} - \lambda_1 \eta x_1(t) u(t) \quad (8)$$

with a constant  $\hat{B} = 0.5 \text{ mm}^3 \cdot \text{h}^{-3}$ .

The practical usability of the theorem depends on its needed measurement frequency for variable  $x_1(t)$ . The worst case corresponds to the  $\delta t = 24 \text{ h}$  cycle time (i.e. to daily measurements). While fixing the times-step of the Euler integration at  $\delta t_{intl} = 1 \text{ h}$ , as  $\delta t$  increases, (7) may become a more or less “corrupted approximation”, a “substitute”, and finally some “surrogate” of the measured 3<sup>rd</sup> time-derivatives. In such cases the serum is injected in the 1<sup>st</sup> step of the Euler integration, and  $u = 0$  in the other segments of this integration. The simulation results obtained for  $\delta t = 24 \text{ h}$  are given in Fig. 4 and 5.

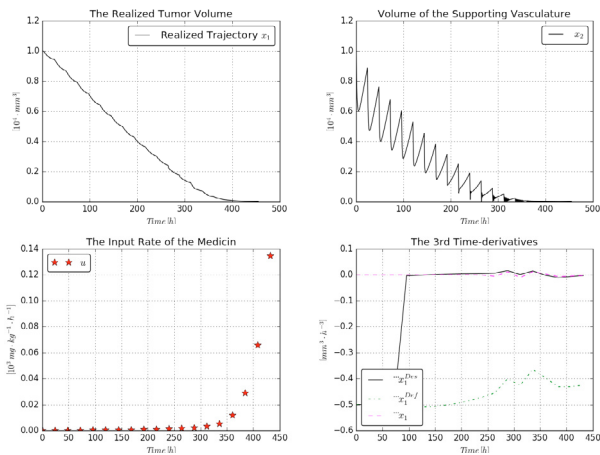


Figure 4. The size of the tumor and its feeding vascular system in the “ $\delta t = 24 \text{ h}$  case”, the ingress rate of the serum Bevacizumab, and the estimated 3<sup>rd</sup> order derivatives

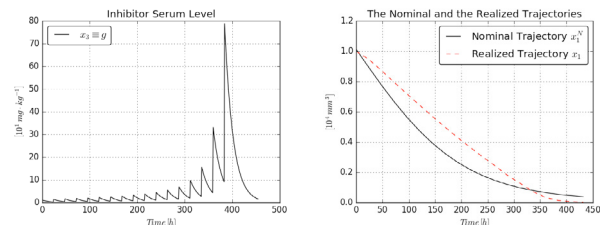


Figure 5. The inhibitor serum level and the trajectory tracking in the “ $\delta t = 24 \text{ h}$  case”

It is evident that during a day-long ( $\delta t = 24 \text{ h}$ ) period, when the serum is injected in the 1<sup>st</sup> hour after the tumor size measurement, the decrease in  $g(t)$  is considerable due to the decay-rate  $\lambda_3$ . This causes fine “ripples” in the tumor volume function  $x_1(t)$ , and an even more visible variation in the volume of the supporting vasculature. As the serum leaves the human body, the process of angiogenesis accelerates.

These effects become more visible for  $\delta t = 72 \text{ h}$  cycle-time in Fig. 6. It is evident that the tumor has enough time for regrowing before the next injection of the serum.

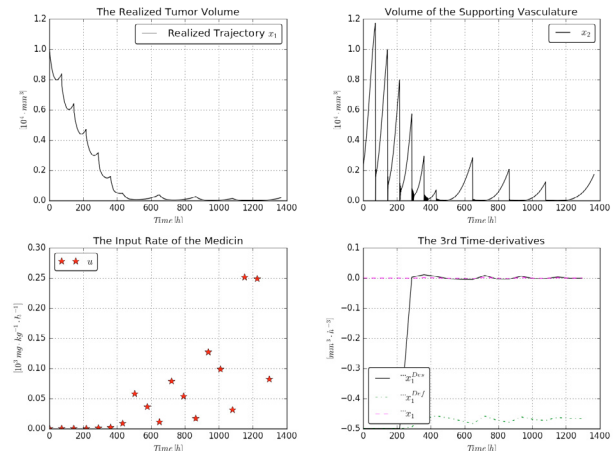


Figure 6. The size of the tumor and its feeding vascular system in the “ $\delta t = 72 \text{ h}$  case”, the ingress rate of the serum Bevacizumab, and the estimated 3<sup>rd</sup> order derivatives

Finally, the weekly treatment would be “ideal”. For this purpose the  $\delta t = 168 \text{ h}$  cycle-time must be used (Fig. 7).

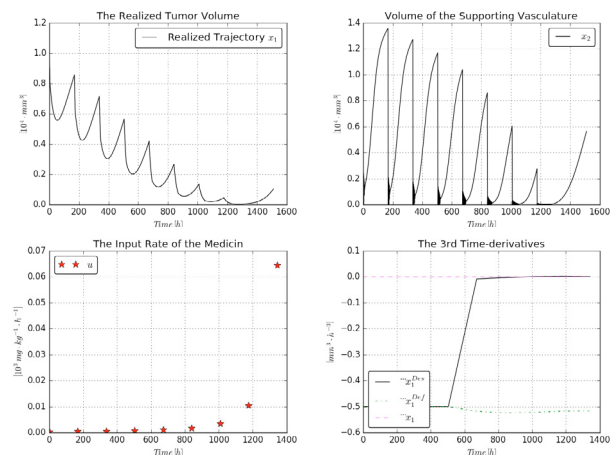


Figure 7. The size of the tumor and its feeding vascular system in the “ $\delta t = 168 \text{ h}$  case”, the ingress rate of the serum Bevacizumab, and the estimated 3<sup>rd</sup> order derivatives

It is evident that during the weekly treatment the supporting vasculature has enough time to grow back, and the tumor also can grow back.

To evade the use of too much serum, in the next simulation we returned to the  $\delta t = 72 \text{ h}$  (3 days) cycle-time, but increasing the allowable “final tumor size” to  $x_{1 \text{ final}} = 10^3 \text{ mm}^3$  (Fig. 8 and 9). According to the simulations this parameter setting seems to be practically acceptable.

Finally, the role of the initial values  $x_1(0)$  and  $x_2(0)$  must be clarified. Due to the 0/0-type singularity in the dynamic model we do not have idea on any interdependence between these variables, as for a given  $x_1(0)$  we have to make calculations for various  $x_2(0)$  values. Let at first consider the pair  $x_1(0) = 10^4 \text{ mm}^3$ ,  $x_2(0) = 10^6 \text{ mm}^3$  (Fig. 10 and 11).

It is interesting to see that in comparison with the Fig. 8 and 9, there is no considerable difference. The huge ini-



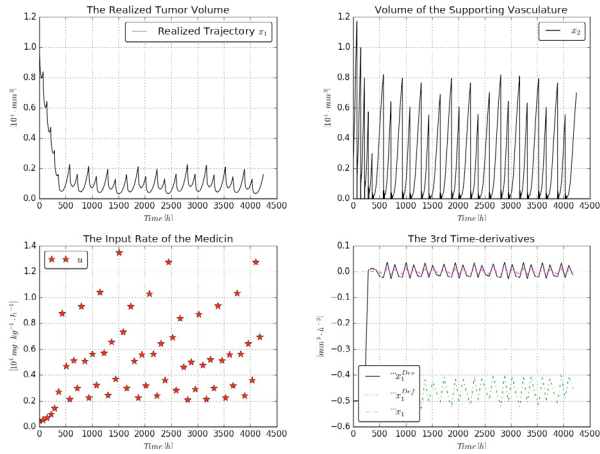


Figure 8. The size of the tumor and its feeding vascular system in the “ $\delta t = 72 \text{ h}$ ,  $x_{1 \text{ final}} = 10^3 \text{ mm}^3$  case”, the ingress rate of the serum Bevacizumab, and the estimated 3<sup>rd</sup> order derivatives

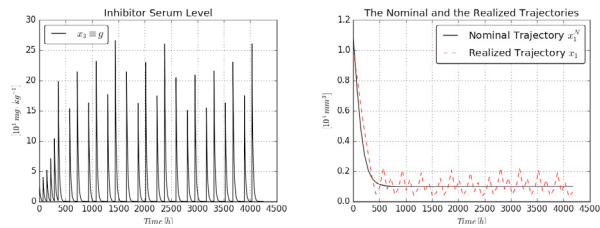


Figure 9. The inhibitor serum level and the trajectory tracking in the “ $\delta t = 72 \text{ h}$ ,  $x_{1 \text{ final}} = 10^3 \text{ mm}^3$  case”

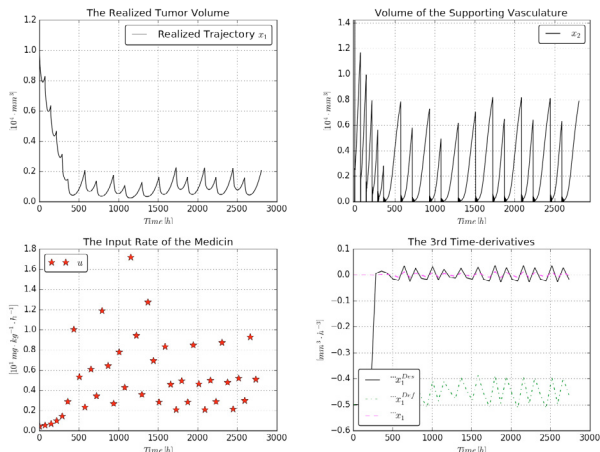


Figure 10. The size of the tumor and its feeding vascular system in the “ $\delta t = 72 \text{ h}$ ,  $x_{1 \text{ final}} = 10^3 \text{ mm}^3$ ,  $x_1(0) = 10^4 \text{ mm}^3$ ,  $x_2(0) = 10^6 \text{ mm}^3$  case”, the ingress rate of the serum Bevacizumab, and the estimated 3<sup>rd</sup> order derivatives

tial vasculature quickly decreases and the injected serum rate is not increased by orders of magnitudes. Secondly, consider the pair  $x_1(0) = 10^4 \text{ mm}^3$ ,  $x_2(0) = 10^2 \text{ mm}^3$  (Fig. 12). Again, the differences between the previously investigated cases and the present one do not seem to be considerable.

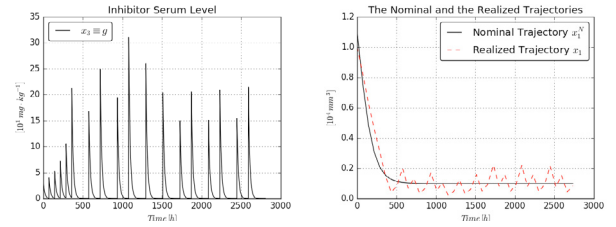


Figure 11. The inhibitor serum level and the trajectory tracking in the “ $\delta t = 72 \text{ h}$ ,  $x_{1 \text{ final}} = 10^3 \text{ mm}^3$ ,  $x_1(0) = 10^4 \text{ mm}^3$ ,  $x_2(0) = 10^6 \text{ mm}^3$  case”

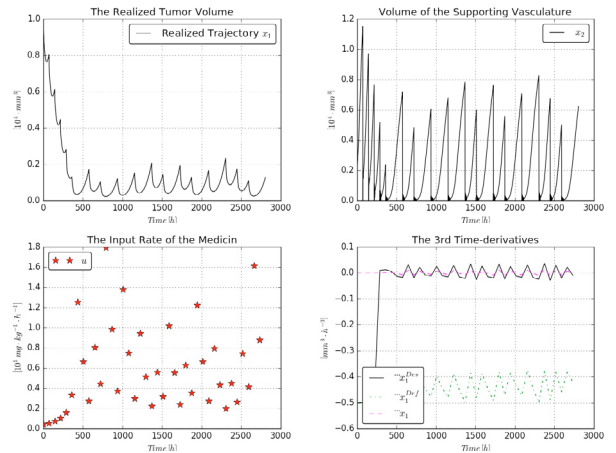


Figure 12. The size of the tumor and its feeding vascular system in the “ $\delta t = 72 \text{ h}$ ,  $x_{1 \text{ final}} = 10^3 \text{ mm}^3$ ,  $x_1(0) = 10^4 \text{ mm}^3$ ,  $x_2(0) = 10^2 \text{ mm}^3$  case”, the ingress rate of the serum Bevacizumab, and the estimated 3<sup>rd</sup> order derivatives

## 5. CONCLUSIONS

In this paper the PD-RFPT-based adaptive control approach was investigated for antiangiogenic tumor growth control on the Hanhfeldt model. The RFPT method is controlled by a single adaptive parameter. Numerical simulations were carried out by the use of the MIT’s Julia package and Euler integration with maximal discrete time-step of  $\delta t_{intl} = 1 \text{ h}$ .

Considering the  $\frac{0}{0}$ -type singularity of the model and the inefficiency of the Bevacizumab serum in inhibiting angiogenesis at very small tumor volumes, a nominal trajectory starting at  $x_1(0) = 10^4 \text{ mm}^3$  and ending at  $x_{1 \text{ final}} = 10^3 \text{ mm}^3$  final tumor volume with  $\delta t = 72 \text{ h}$  sampling and treating (serum injection) frequency can be suggested as an “acceptable” compromise. It was presented that the initial volume of the supporting vasculature  $x_2(0) \in [10^2, 10^6] \text{ mm}^3$  surprisingly does not seem to have significant effects on the results.

It should be noted that the suggested control is based only on the measurement of the tumor volume variable  $x_1(t)$  in the sampling times, and does not need the estimation or measurement of the state variables  $x_2(t)$  and  $x_3(t)$ . Instead of that it uses a simple “affine model” defined in (8), that contains a simple constant instead of the “exact contributions” that are very complicated functions of the

state variables. This fact has a great practical advantage. Although the suggested control has the relative order 3, it was found that it can use the very rough estimation or “surrogate” of  $\tilde{x}_1$  on the basis of the simple estimation defined in (7).

Regarding further researches, it seems to be expedient investigating the available other models of cancer treatment applying angiogenic inhibition mechanisms.

#### ACKNOWLEDGEMENTS

The authors thankfully acknowledge the support of the Research, Innovation and Service Center of Óbuda University, Budapest, Hungary.

#### REFERENCES

- Banach, S. (1922). Sur les opérations dans les ensembles abstraits et leur application aux équations intégrales (About the Operations in the Abstract Sets and Their Application to Integral Equations). *Fund Math*, 3, 133–181.
- Charlton, P. and Spicer, J. (2016). Targeted therapy in cancer. *Medicine*, 44(1), 34–38.
- Czakó, B., Sági, J., and Kovács, L. (2017). Model-based optimal control method for cancer treatment using model predictive control and robust fixed point method. *In Proc. of the 21st International Conference on Intelligent Engineering Systems (INES 2017), Larnaca, Cyprus*, 271–276.
- Deuffhard, P. (2004). *Newton Methods for Nonlinear Problems. Affine Invariance and Adaptive Algorithms*, Springer Series in Computational Mathematics, Vol. 35. Springer, Berlin.
- Dineva, A., Tar, J., Vákonyi-Kóczy, A., and Piuri, V. (2016). Adaptive controller using Fixed Point Transformation for regulating propofol administration through wavelet-based anesthetic value. *In Proc. IEEE International Symposium on Medical Measurements and Applications (MeMeA 2016), Benevento, Italy*, 650–655.
- Distler, J., Hirth, A., Kurowska-Stolarska, M., Gay, R., Gay, S., and Distler, O. (2003). Angiogenic and angiostatic factors in the molecular control of angiogenesis. *Quart J Nuclear Med*, 47(3), 149–161.
- Drexler, D., Sági, J., and Kovács, L. (2017a). Potential Benefits of Discrete-Time Controller-based Treatments over Protocol-based Cancer Therapies. *Acta Pol Hung*, 14(1), 11–23.
- Drexler, D., Sági, J., and Kovács, L. (2017b). Modeling of tumor growth incorporating the effects of necrosis and the effect of bevacizumab. *Complexity*, 1–10.
- Drexler, D., Sági, J., and Kovács, L. (2017c). A minimal model of tumor growth with angiogenic inhibition using Bevacizumab. *In Proc. of the IEEE 15th International Symposium on Applied Machine Intelligence and Informatics (SAMi 2017), January 26-28, 2017, Herl'any, Slovakia*, 185–190.
- Eigner, G., Horváth, P., Tar, J., Rudas, I., and Kovács, L. (2015). Application of Robust Fixed Point control in case of T1DM. *In Proc. of the IEEE International Conference on Systems, Man, and Cybernetics (IEEE SMC 2015), Hong Kong, China*, 2459–2464.
- Grancharova, A. and Johansen, T. (2012). *Explicit Non-linear Model Predictive Control*. Springer.
- Grüne, L. and Pannek, J. (2011). *Nonlinear Model Predictive Control*. Springer.
- Hanhfeldt, P., Panigrahy, D., Folkman, J., and Hlatky, L. (1999). Tumor development under angiogenic signaling: A dynamical theory of tumor growth, treatment response, and postvascular dormancy. *Bul Mathem Biology*, 59(19), 4470–5.
- Harris, A. (2003). Angiogenesis as a new target for cancer control. *Europ J Cancer Suppl*, 1(2), 1–12.
- Ilic, I., Jankovic, S., and Ilic, M. (2016). Bevacizumab combined with chemotherapy improves survival for patients with metastatic colorectal cancer: Evidence from meta-analysis. *PLoS ONE*, 11(8), e0161912.
- Ionescu, C., Lopes, A., Copot, D., Machado, J., and Bates, J. (2017). The role of fractional calculus in modeling biological phenomena: A review. *Communications in Nonlinear Science and Numerical Simulation*, 51, 141–159.
- Kelley, C. (2003). *Solving Nonlinear Equations with Newton's Method, no 1 in Fundamentals of Algorithms*. SIAM.
- Klamka, J., Maurer, H., and Swierniak, A. (2017). Local controllability and optimal control for a model of combined anticancer therapy with control delays. *Math Biosci Eng*, 14(1), 195–216.
- Kovács, L. (2017). A robust fixed point transformation-based approach for type 1 diabetes control. *Nonlin Dynamics*, 89, 2481–2493.
- Ledzewicz, U. and Schättler, H. (2005). A synthesis of optimal controls for a model of tumor growth under angiogenic inhibitors. *In Proc. 44th IEEE Conference on Decision and Control, and the European Control Conference (IEEE CDC-ECC 2005, Seville, Spain)*, 934–939.
- Levant, A. (1998). Arbitrary-order sliding modes with finite time convergence. *In Proc. 6th IEEE Mediterranean Conference on Control and Systems (MED 1998), Alghero, Italy*, 349–354.
- Lobato, F., Machado, V., and Steffen, V. (2016). Determination of an optimal control strategy for drug administration in tumor treatment using multi-objective optimization differential evolution. *Comp Meth Prog Biomed*, 131, 51–61.
- Michelson, S. and Leith, J. (1997). Positive feedback and angiogenesis in tumor growth control. *Bul Mathem Biology*, 59(2), 233–254.
- Tar, J., Bitó, J., Nádai, L., and Tenreiro Machado, J. (2009). Robust Fixed Point Transformations in adaptive control using local basin of attraction. *Acta Pol Hung*, 6(1), 21–37.
- Vasudev, N. and Reynolds, A. (2014). Anti-angiogenic therapy for cancer: Current progress, unresolved questions and future directions. *Angiogenesis*, 17(3), 471–494.
- Ypma, T.J. (1995). Historical development of the Newton-Raphson method. *SIAM Review*, 37(4), 531–551.
- Zhou, Y., Ionescu, C., and Machado, J.T. (2015). *Fractional dynamics and its applications*. Springer.